Catalysis Today xxx (xxxx) xxx–xxx

Contents lists available at ScienceDirect

Catalysis Today

journal homepage: www.elsevier.com/locate/cattod

Investigation of metal oxide additives onto Na_2WO_4-Ti/SiO_2 catalysts for oxidative coupling of methane to value-added chemicals

Sarannuch Sringam[a], Phattaradit Kidamorn[a], Thanaphat Chukeaw[a,b], Metta Chareonpanich[a,b,c], Anusorn Seubsai[a,b,c,*]

[a] Department of Chemical Engineering, Faculty of Engineering, Kasetsart University, Bangkok, 10900, Thailand
[b] Center of Excellence on Petrochemical and Materials Technology, Kasetsart University, Bangkok, 10900, Thailand
[c] Research Network of NANOTEC–KU on NanoCatalysts and NanoMaterials for Sustainable Energy and Environment, Kasetsart University, Bangkok, 10900, Thailand

ARTICLE INFO

Keywords:
Catalyst
Manganese oxide
Oxidative coupling of methane
Sodium tungstate
Titanium dioxide

ABSTRACT

The oxidative coupling of methane (OCM) is a closely related reaction process involving the transformation of methane (CH_4) and O_2 mixtures into value-added chemicals such as ethylene and ethane (i.e. C_{2+}). This work presents the effects of metal oxide additives into the Na_2WO_4-Ti/SiO_2 catalyst on the performance of the OCM reaction. Several metal oxide additives—including oxides of Co, Mn, Cu, Fe, Ce, Zn, La, Ni, Zr, Cr, and V—were investigated with the Na_2WO_4-Ti/SiO_2 catalyst. All of the catalysts were prepared using co-impregnation and the catalyst activity test was performed in a plug flow reactor at a reactor temperature range of 600–800 °C and atmospheric pressure. The physicochemical properties of the prepared catalysts relating to their catalytic activity were discussed by using the information of X-ray diffraction (XRD), X-ray photoelectron spectroscopy (XPS), and scanning electron microscopy (SEM) measurements. Na_2WO_4-Ti/SiO_2 added Mn was found to be the most active catalyst, involving shifts of binding energies of W 4f and Ti 2p toward lower binding energies. Moreover, a variety of operating conditions—including reactant- to-nitrogen gas ratio, catalyst mass, reactor temperature, and total feed flow rate—were intensively examined for the OCM reaction using the Na_2WO_4-Ti-Mn/SiO_2 catalyst. The maximum C_{2+} yield was subsequently discovered at 22.09% with 62.3% C_{2+} selectivity and 35.43% CH_4 conversion. Additionally, the stability of the Na_2WO_4-Ti-Mn/SiO_2 catalyst was also monitored with time on stream for 24 h.

1. Introduction

Methane (CH_4) is the primary component of natural gas and biogas. It is considered a greenhouse gas about 25 times stronger than CO_2 if these two gases are released to the atmosphere in the same amount [1]. Since CH_4 is abundant on Earth, it is highly attractive to worldwide researchers to explore strategies to transform it into more useful products. One of the most challenging methods is the oxidative coupling of methane (OCM), which is a type of chemical reaction using air or oxygen directly reacting with CH_4 to produce useful hydrocarbons such as ethylene, ethane, propene, propane, etc. (C_{2+}) [2–5]. In the absence or presence of a catalyst, the OCM reaction is exothermic and normally takes place in reaction temperatures of 600–1,000 °C [6]. Moreover, CO and CO_2 can be produced as byproducts. However, it is believed that if a suitable catalyst is present, the products can be controlled and the extreme reaction temperature can be reduced.

Previously, several potential catalysts have been reported for the OCM reaction to C_{2+}, especially Mn modified with a variety of co-catalysts, supports, and/or promoters, such as oxides of Mg, Na, and Ce. The activity of those catalysts was approximately < 16% C_{2+} yield and 25–78% C_{2+} selectivity. Lately, a solid mixture of Na_2WO_4-Mn supported on SiO_2 has been greatly attractive to researchers worldwide, because this combination is highly active for the OCM reaction. The catalyst has also been modified with many metals (e.g. Li, Na, K, Ba, Ca, Fe, Co, Ni, Al, Ti, Ce, etc.) [7–9]. Some of these modified catalysts, especially Na_2WO_4-Mn/SiO_2 doped with TiO_2 [10,11], exhibited an improvement on both C_{2+} yield and selectivity (i.e. 16.8% C_{2+} yield and 73% C_{2+} selectivity). The addition of a promoter into the Na_2WO_4-Mn/SiO_2 catalyst (e.g. LiCl, NaCl, KCl, or CsCl) has also been found to result in the incorporation of the promoter into the catalytic material, thus increasing the number of strong basic sites, thereby enhancing the catalyst activity [12–14].

Recently, we have found a combination of Na_2WO_4 and Ti-supported SiO_2 exhibiting high activity for the OCM reaction, giving 4.9%

* Corresponding author at: Department of Chemical Engineering, Faculty of Engineering, Kasetsart University, Bangkok, 10900, Thailand.
E-mail address: fengasn@ku.ac.th (A. Seubsai).

https://doi.org/10.1016/j.cattod.2020.03.048
Received 2 March 2019; Received in revised form 19 February 2020; Accepted 25 March 2020

C_{2+} yield with 71.7% C_{2+} selectivity and 6.8% CH_4 conversion at a reactor temperature of 700 °C and atmospheric pressure [15]. The activity of the catalyst had good stability over 24 h of on-stream testing. Moreover, a crystalline structure of α-cristobalite of SiO_2 that was present along with TiO_2 crystals was found to substantially enhance the activity of the catalyst for the OCM reaction to C_{2+}. Therefore, improve the activity of this catalyst is of great interest. Herein, we modify the catalyst by adding a metal oxide additive into the Na_2WO_4-Ti/SiO_2 catalyst. The selected metal oxide additives include Co, Mn, Cu, Fe, Ce, Zn, La, Ni, Zr, Cr, and V. The most active catalyst is subsequently chosen to optimize the C_{2+} yield by varying operating conditions. Additionally, advanced instrument techniques are also used to analyze the prepared catalysts to acquire their physicochemical properties to relate with their catalytic activity.

2. Experimental

2.1. Catalyst preparation

All of the catalysts were prepared using co-impregnation as follows. Weights of Na_2WO_4 (Na_2WO_4•$2H_2O$, 98.0 ~ 101.0%, Daejung), Ti ($C_{12}H_{28}O_4Ti$, 97 + %, Alfa Aesar), and X (X = Co, Mn, Cu, Fe, Ce, Zn, La, Ni, Zr, Cr, or V) were determined and pipetted from each stock precursor solution into amorphous fume SiO_2 (surface area of 85-115 m^2/g, Alfa Aesar) to obtain a desired weight percentage of the metal components. Note that the precursor of the 11 elements was in the form of metal nitrate hydrate, and the weight percentage of each component on the support was calculated based on the formula appearing in each catalyst's name. For example, for the Na_2WO_4-Ti-Mn/SiO_2 catalyst, the weights of Na_2WO_4, Ti(0), and Mn(0) were determined and loaded onto the SiO_2 support. After that, the mixture was stirred at room temperature for 2 h and heated to 120 °C until dried. Then, the dried powder was set to calcine in an air furnace at 800 °C for 4 h. Finally, the powder was ground until a fine powder was obtained. The weight percentage of each component for each catalyst will be elaborated in the results and discussion of that mentioned figure.

2.2. Catalytic activity test

The activity of each prepared catalyst for the OCM reaction was evaluated in a plug flow reactor at atmospheric pressure. The reactor temperature was set in the range of 600–800 °C. A catalyst (8–72 mg) was packed in a quartz tube reactor (0.5 cm inner diameter) and sandwiched between layers of quartz wool. The feed gas consisted of methane (CH_4, 99.999%, Praxair), oxygen (O_2, 99.999%, Praxair), and nitrogen (N_2, 99.999%, Praxair) at a volume ratio of CH_4:O_2:N_2 = 3:1:0, 3:1:2, or 3:1:4 with a total feed flow rate in the range of 35–95 mL/min. The effluent gas was evaluated using an online gas chromatograph (SHIMADZU, GC-14A) equipped with a flame ionization detector (FID; for analyzing C_2H_4, C_2H_6, C_3H_6, C_3H_8 and C_4H_8, and C_4H_{10}) and a thermal conductivity detector (TCD; for analyzing CO, CO_2, and CH_4). The activity of each catalyst was analyzed after the system had reached a set point of 2 h. Equations (1)–(4) show the formulas for calculating the %CH_4 conversion, %C_{2+} selectivity, %CO_x selectivity, and %C_{2+} yield.

$$\%\,CH_4\ \text{conversion} = \frac{\text{moles of } CH_4 \text{ input} - \text{moles of } CH_4 \text{output}}{\text{moles of } CH_4 \text{ input}} \times 100 \quad (1)$$

$$\%\,C_{2+}\ \text{selectivity} = \frac{\text{moles of } C_{2+}}{\text{Total moles of products}} \times 100 \quad (2)$$

$$\%\,CO_x\ \text{selectivity} = \frac{\text{moles of } CO_x}{\text{Total moles of products}} \times 100 \quad (3)$$

$$\%\,C_{2+}\ \text{yield} = \frac{\%\,CH_4\ \text{conversion} \times \%\,C_{2+}\text{selectivity}}{100} \quad (4)$$

2.3. Catalyst characterization

The X-ray diffraction (XRD) patterns of each catalyst were obtained using a powder X- ray diffractometer (PXRD; JEOL JDX-3530 and Philips X-Pert, using Cu-K_α radiation, 45 kV and 40 mA). The electronic states of selected elements in each catalyst were examined using X-ray photoelectron spectroscopy (XPS; Kratos Axis Ultra DLD) with Al Kα for the X-ray source. The surface morphology of the samples was imaged using a scanning electron microscope (SEM, FE-SEM: JEOL JSM7600 F).

3. Results and discussion

3.1. Activity of Na_2WO_4-Ti/SiO_2 added metal oxide additives

In catalyst screening experiments for the OCM reaction in our laboratory, we have found that 5 wt% Na_2WO_4 + 5 wt% Ti on SiO_2 (denoted as Na_2WO_4-Ti/SiO_2) showed a priming result for C_{2+} production. We also found, from an XPS measurement of the catalyst, that the form of Ti was TiO_2 (data are not shown here). In this work, the Na_2WO_4-Ti/SiO_2 catalyst was further investigated by adding 11 elements, Co, Mn, Cu, Fe, Ce, Zn, La, Ni, Zr, Cr, and V. These 11 elements were selected from the transition metals because of their availability, non-toxicity, inexpensiveness, and, more importantly, inactiveness for CH_4 combustion [16]. All of the Na_2WO_4-Ti/SiO_2 catalysts with added metal oxide additive were prepared using a metal ratio of Na_2WO_4:Ti:X = 5:5:2 (where X is an metal oxide additive and its weight is calculated on the basis of the metallic form). The total metal loading was 12 wt% for every catalyst, except Na_2WO_4-Ti/SiO_2 (i.e. 5 wt% Na_2WO_4 + 5 wt % Ti). The activity test results of the catalysts are presented in Fig. 1.

Under the same testing conditions, the catalyst without metal oxide additive exhibited 4.43% C_{2+} yield with 33.8% C_{2+} selectivity and 13.34% CH_4 conversion. The most promising catalyst was the addition of Mn into the Na_2WO_4-Ti/SiO_2 catalyst, yielding 9.97% with 35.0% C_{2+} selectivity and 29.48% CH_4 conversion. The other metal oxides, which were added into the Na_2WO_4-Ti/SiO_2 catalyst and gave a C_{2+} yield higher than that of the catalyst without metal oxide additive, were (in order) Co > Fe > Ce > Zn, giving C_{2+} yield in a range of 4.50–7.65%. The addition of Mn clearly greatly improved the activity of

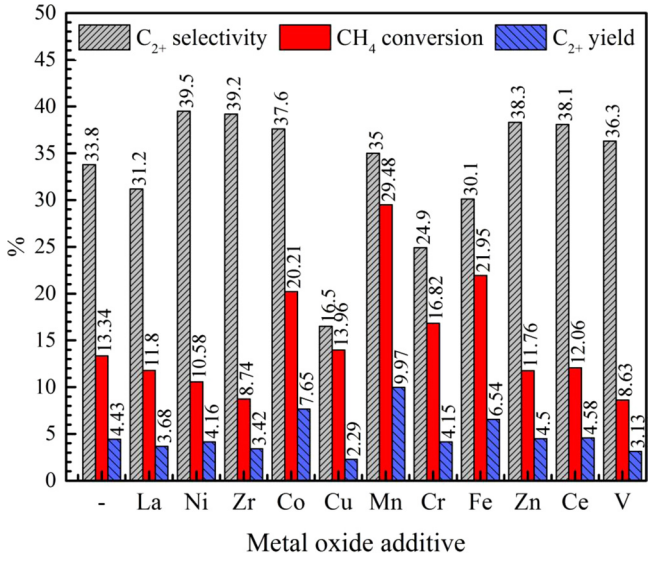

Fig. 1. Catalyst activity of Na_2WO_4-Ti/SiO_2 added metal oxide additives. Reaction conditions: CH_4:O_2:N_2 ratio = 3:1:0, catalyst weight = 8 mg, total feed flow rate of 35 mL/min, reactor temperature = 700 °C.

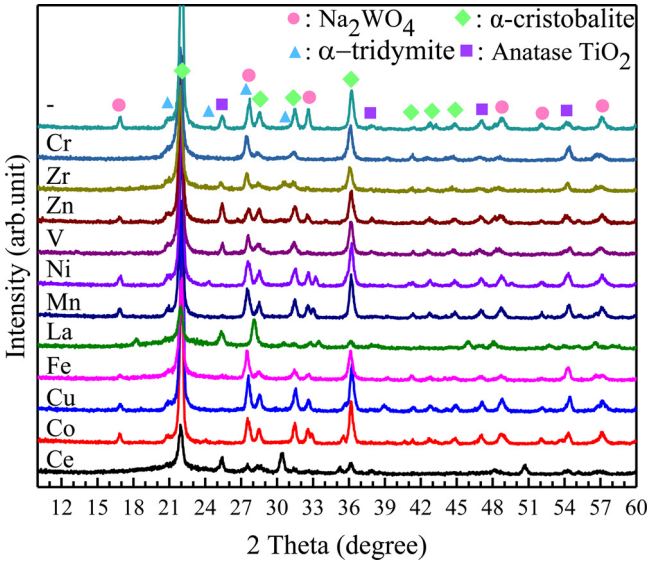

Fig. 2. XRD patterns of Na_2WO_4-Ti/SiO_2 catalyst added metal oxide additives, fixing wt% of Na_2WO_4:Ti:X = 5:5:2 and SiO_2 balance.

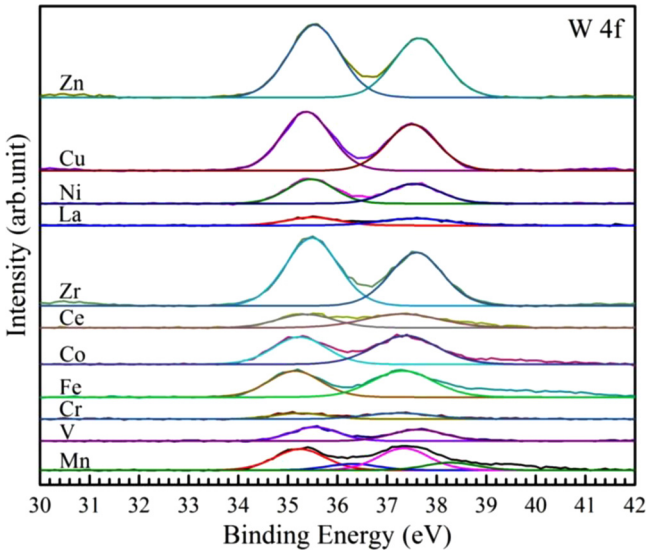

Fig. 3. XPS spectra of Na_2WO_4-Ti/SiO_2 added different metal oxide additives showing binding energy in the range of W4f.

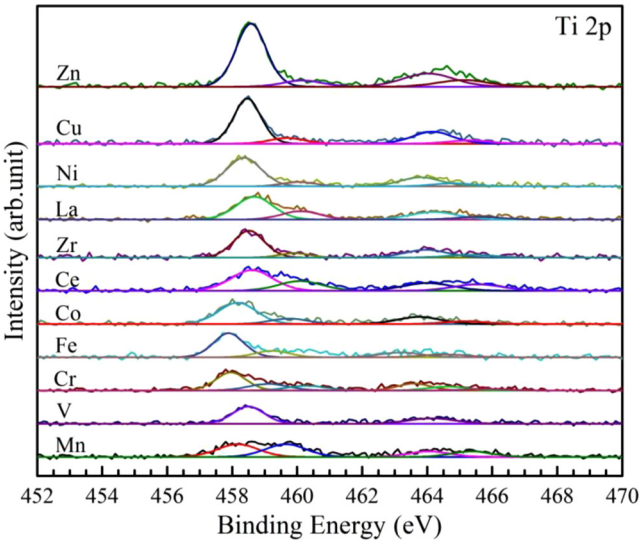

Fig. 4. XPS spectra of Na_2WO_4-Ti/SiO_2 added different metal oxide additives showing binding energy in the range of Ti2p.

Na_2WO_4-Ti/SiO_2. The characterization using XRD and XPS of these catalysts will reveal how the activities of some catalysts improve, which will be presented in the next section.

3.2. XRD and XPS analyses of Na_2WO_4-Ti/SiO_2 added metal oxide additives

XRD patterns of the Na_2WO_4-Ti/SiO_2 catalysts with added metal oxide additives are presented in Fig. 2. The characteristic peaks of *α*-cristobalite (2θ = 22.1, 28.6, 31.5, 36.1, 41.2, 42.9, and 44.9 (ICDD No. 00-001-0438)) appeared for all catalysts. A small XRD peak indicating the presence of *α*-tridymite (2θ = 21.8, 23.3, 27.3, and 30.1 (ICDD No. 00-003-0227)) was also observed. The characteristic peaks of Na_2WO_4 (16.9, 27.8, 32.4, 48.8, 52.1, and 57.1 (ICDD No. 01-074-2369)) appeared in the Na_2WO_4 catalysts with no added (-), Zn, Ni, Mn, Fe, Cu, and Co. The characteristic peaks of TiO_2 (2θ = 25.2, 37.0, 48.0, 54.1, and 55.0 (ICDD No. 01-073-1764)) were seen in the Na_2WO_4 catalysts with no added (-), Zr, Zn, V, La, and Ce. It should be noted that the most active catalyst presented in Fig. 1 was Na_2WO_4-Ti-Mn/SiO_2. As shown in Fig. 2, this catalyst consisted of *α*-cristobalite, crystalline Na_2WO_4, and crystalline Mn_2O_3 (2θ = 33.1, 38.1, and 44.8 (ICDD No. 00-002-0896)). Hence, the presence of these crystalline phases is essential for the OCM reaction. For the role of Ti, its combination with Mn has been proposed in the form of the $MnTiO_3$ phase; then, the $MnTiO_3$ phase plays an important role in remarkably improving the catalyst activity [10,11]. However, no XRD peaks of $MnTiO_3$ can be observed in Fig. 2, probably because a small amount of Mn was loaded and/or the crystal species is too small to be detected.

The XPS spectra of all catalysts in the range of W (4f) and Ti (2p) regions are presented in Figs. 3 and 4, respectively. The observed peaks corresponded to WO_42-($4f_{5/2}$ ~ 37.6 eV, $4f_{7/2}$ ~ 35.4 eV) and TiO_2 ($2p_{1/2}$ ~ 464 eV, $2p_{3/2}$ ~ 459 eV). Of interest was that the peaks of $WO_42-$and TiO_2 of each catalyst were not identical. Perhaps, the addition of metal oxides influences the interaction of WO_4-2 or Ti bonding with O2−, thus leading to shifts of the binding energies [17–19].

The most interesting results are presented in Fig. 5, showing the plots of CH_4 conversion of each catalyst versus its binding energy of W $4f_{7/2}$ (Fig. 5a) and Ti $2p_{3/2}$ (Fig. 5b). The plots in each figure can be divided into two groups: group 1 (the catalysts containing Mn, Fe, Co, and Cr) and group 2 (the catalysts containing Cu, Zn, Ce, La, Ni, Zr, and V). The catalysts in group 1 possessed binding energies in a range of 35.12–35.24 eV for W $4f_{7/2}$ and 457.90–458.20 eV for Ti $2p_{3/2}$, while the catalysts in group 2 gave the XPS signal in a range of 35.36–35.56 eV for W $4f_{7/2}$ and 458.34–458.68 eV for Ti $2p_{3/2}$. It is interesting to see that the CH_4 conversions of the catalysts in group 1 were significantly higher than those in group 2. Moreover, the catalysts in group 1 clearly exhibited binding energies lower than the catalysts in group 2. Importantly, these findings suggest that the metal additives—that are able to shift the binding energies of W 4f and Ti 2p toward lower binding energies when added into the Na_2WO_4-Ti/SiO_2 catalyst—are highly active for the OCM reaction.

It is possible that when the binding energy of W 4f or Ti 2p shifts toward a lower binding energy, the energy to remove an electron from the outer electron layer of W or Ti will become lower [18]. This reveals that it becomes easier for an oxygen atom bonding with W or Ti to dissociate or leave from the center. In other words, when an oxygen molecule adsorbs onto an active site—WO_4^{2-} associated with Ti^{2+}—it will dissociate and bond with the center of W or Ti. Due to the influence of a metal oxide additive added into the catalyst, the oxygen atom can easily detach from and leave the active metal center as H_2O [18]. This

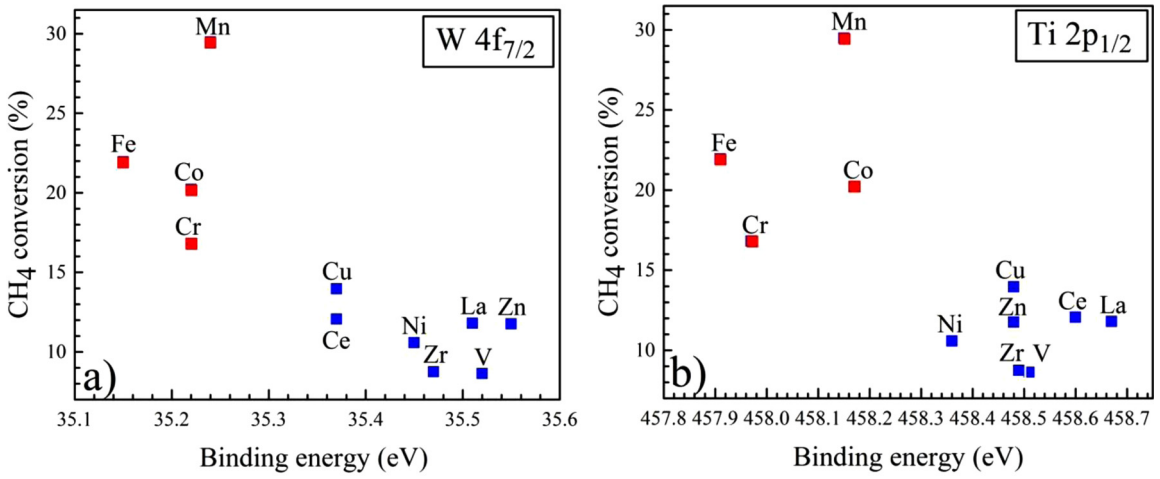

Fig. 5. Plots of correlation between CH_4 conversions and binding energies of a) W $4f_{7/2}$ and b) Ti $2p_{1/2}$.

proposed behavior can significantly enhance the reaction mechanism for OCM. As a result, the catalysts in group 1 exhibit a higher CH_4 conversion relative to those in group 2. Future studies, to deeply understand the reaction mechanism, are required.

3.3. Optimization of Na_2WO_4-Ti-Mn/SiO_2 catalyst for production of C_{2+}

The Na_2WO_4-Ti-Mn/SiO_2 catalyst was further optimized to increase C_{2+} yield by first varying the weight percentage of Mn into Na_2WO_4-Ti/SiO_2 from 0.0 to 2.5 wt%. The results are shown in Fig. 6. The C_{2+} yield was found to be optimized at 0.5 wt% Mn loading (12.16% C_{2+} yield with 39.7% C_{2+} selectivity and 30.62% CH_4 conversion, then the C_{2+} yields slightly decreased to approximately 9.6%). The decrease in the activity of the catalysts with Mn loading over 0.5 wt% could be due to the formation of MnO_x multilayers, which affects the generation of nucleophilic oxy species (e.g. O_2–, O_2^{2-}, and O–) [20]. SEM images of the catalysts shown in Fig. 6 are illustrated in Fig. 7. As shown, the surface morphology and particle size of all catalysts are similar. All the particles are irregularly shaped with various sizes, ranging from 50 nm to about 1 μm in diameter of coral reef-shaped particles. Nevertheless, the catalytic activity of each catalyst is different, probably due to differences in the distribution of the active Mn species (Mn_2O_3, $MnTiO_3$) in each catalyst.

The best Na_2WO_4-Ti-Mn/SiO_2 catalyst found in Fig. 6 was further

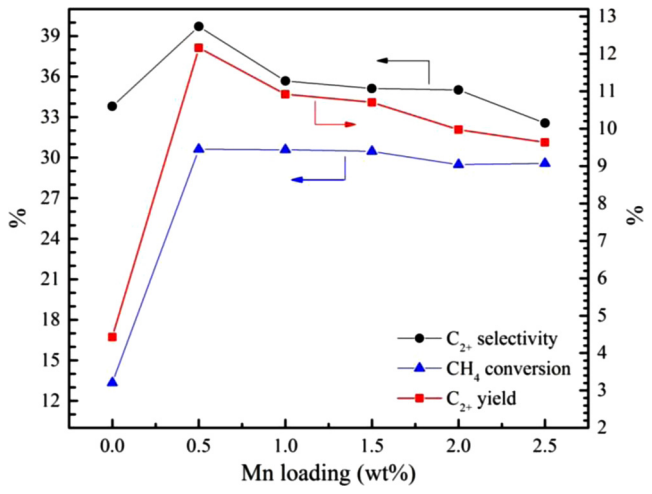

Fig. 6. Effect of Mn loading into Na_2WO_4-Ti/SiO_2. Reaction conditions: CH_4:O_2:N_2 ratio = 3:1:0, catalyst weight = 8 mg, total feed flow rate of 35 mL/min, reactor temperature = 700 °C.

investigated by varying catalyst amounts and reactant gas feeding ratios, while the total feed flow rate was fixed at 35 mL/min for every condition. Three reactant gas feeding ratios of CH_4:O_2:N_2 were used, including CH_4:O_2:N_2 = 3:1:0, 3:1:2, and 3:1:4. The results are plotted in Fig. 8. As expected, the activity of the catalyst increased on increasing the catalyst amount because the number of active sites increase as the catalyst amount increases. Consequently, more CH_4 can react with the active sites, thereby increasing the C_{2+} yields. The catalyst amount of each reactant gas feeding ratio that delivered the highest C_{2+} yield was 24, 48, and 64 mg, giving a C_{2+} yield of 19.19%, 19.61%, and 18.70% when the reactant gas feeding ratio of CH_4:O_2:N_2 was 3:1:0, 3:1:2, and 3:1:4, respectively. It should be noted that the optimal point of each condition is the point where the O_2 gas is completely consumed. Thus, after the optimal points, the CH_4 conversions should have been steady. However, the C_{2+} conversions minimally decreased with gradual decreases of C_{2+} yields, potentially because the C_{2+} products can further react with some special active sites to produce CO, CO_2, and even CH_4 [21–27]. Thus, the CH_4 conversion decreased as the catalyst amount increased.

The optimal catalyst amount of each condition found in Fig. 8 was selected to study the effect of reactor temperature at three different CH_4:O_2:N_2 feeding gas ratios, as shown in Fig. 9. For every feeding gas ratio, the C_{2+} selectivities, CH_4 conversions, and C_{2+}yields increased with increase in reactor temperatures, reaching an optimal value at 700 °C. The highest C_{2+} yield was achieved at 19.61% with 60.40% C_{2+} selectivity and 32.48% CH_4 conversion when the CH_4:O_2:N_2 feeding gas ratio was 3:1:2. At reactor temperatures above 700 °C, the catalyst activity for C_{2+} formation rapidly dropped, while the CH_4 conversions slowly decreased. It is possible that the C_{2+} products quickly combust in the presence of O_2 or react further easily with active sites at high reactor temperatures. Similar to the results in Fig. 8, the slow decreases of CH_4 conversion as reactor temperature rose were due to the additional CH_4 from the decomposition of C_{2+} [17,28–31].

In general, a fuel-rich condition (i.e. CH_4:O_2 ratio > 1.0) is more favorable for C_{2+} production in the OCM reaction. The complete combustion of CH_4 is strongly favorable under fuel-lean conditions. Therefore, the effect of CH_4:O_2 ratio on the activity of the optimal catalyst was studied, as shown in Fig. 10. The CH_4:O_2 ratios were varied from 1.0 to 3.0, for which the conditions ranged from fuel-lean to fuel-rich. The results evidently showed that the C_{2+} yields slowly increased as the CH_4:O_2 ratios were lowered. In other words, O_2 increases into the feed resulted in increases of C_{2+} yields and CH_4 conversions. Nonetheless, the C_{2+} selectivities significantly decreased. The results suggest that O_2 increases into the feed enhance the formations of CO and CO_2 more than those of C_{2+} products [9,26,27].

The effect of total feed flow rate of the Na_2WO_4-Ti-Mn/SiO_2 catalyst

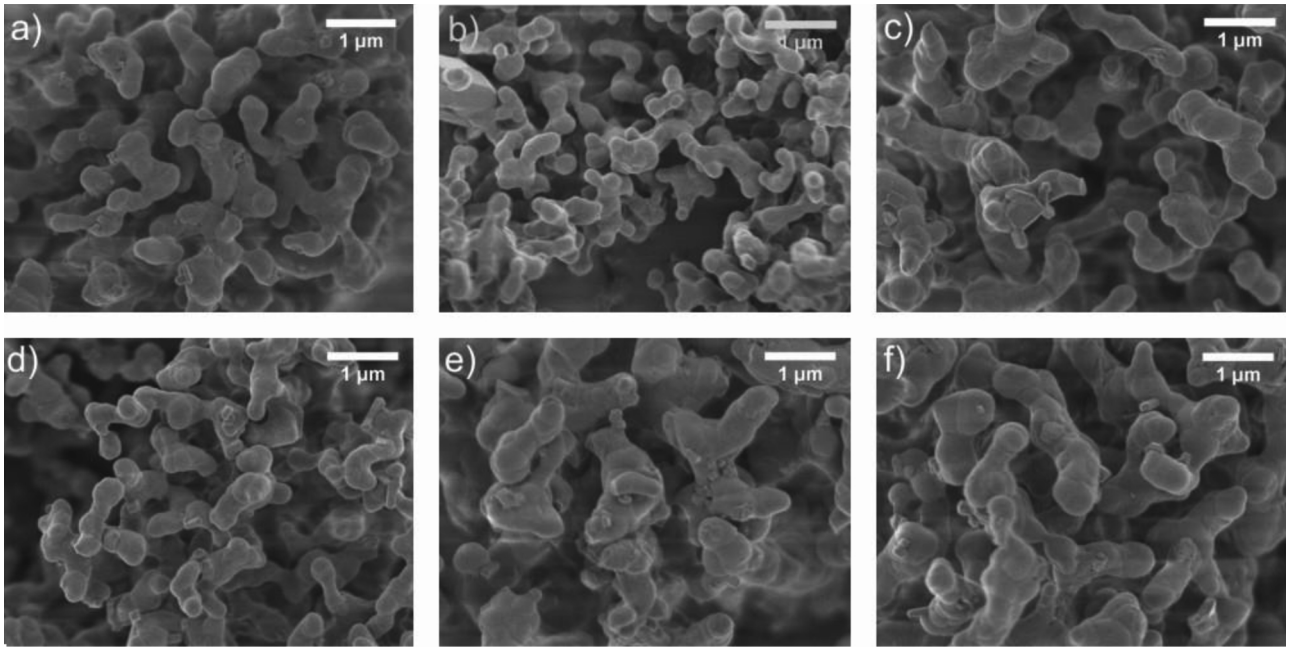

Fig. 7. SEM images of Na_2WO_4-Ti-Mn/SiO_2 catalysts at different Mn loadings: a) 0 wt%, b) 0.5 wt%, c) 1.0 wt%, d)1.5 wt%, e) 2.0 wt%, and f) 2.5 wt%.

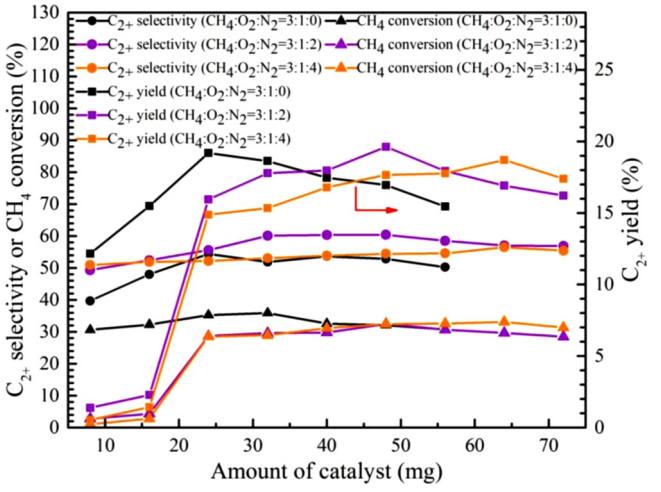

Fig. 8. Activity of Na_2WO_4-Ti-Mn/SiO_2 catalyst at different catalyst amounts and different CH_4:O_2:N_2 feeding gas ratios.

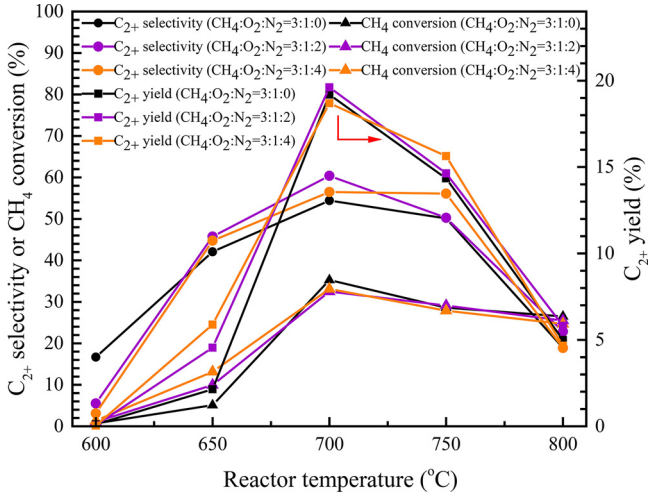

Fig. 9. Activity of Na_2WO_4-Ti-Mn/SiO_2 catalyst at different reactor temperatures and different CH_4:O_2:N_2 feeding gas ratios. Reaction conditions: catalyst weight = 24, 48, and 64 mg for CH_4:O_2:N_2 = 3:1:0, 3:1:2, and 3:1:4, respectively, total feed flow rate =35 mL/min.

for OCM reaction was also investigated as presented in Fig. 11. In general, a short resident time inside a porous catalyst favors C_{2+} selectivity because it reduces chances of combustion of C_{2+} products. The results remarkably showed that the C_{2+} yields and selectivities were achieved at approximately 20–22% and 60–62%, respectively, while the CH_4 conversions were slightly changed at approximately 32–35% when the total feed flow rate was in the range of 45–75 mL/min. At above 75 mL/min, the activity of the catalyst slowly decreased, potentially because the residence time or the contact time between the reactants and the catalyst was greatly reduced.

Lastly, a time-on-stream experiment over 24 h of the Na_2WO_4-Ti-Mn/SiO_2 catalyst at the optimized operating conditions was conducted to monitor its catalyst stability. The plots are presented in Fig. 12. It was found that the CH_4 conversions and the C_{2+} yields slightly decreased from the second to the last hour, while the C_{2+} selectivity remained virtually unchanged. The C_{2+} yield was reduced from 21 to 16% within 24 h of experiment. The catalyst used for 24 h was then observed to examine why the catalyst deactivated using SEM and XRD analyses, as shown in Fig. 13. Apparently, the particle sizes of the used catalyst were much larger (about 50 times) than those of the fresh catalyst. This indicated that one possible cause of the gradual deactivation of the catalyst was the aggregation of the particles (i.e. catalyst sintering). Comparison of the XRD spectra of the fresh and used catalysts shows that the peaks of α-tridymite (2θ = 21.8, 23.3, 27.3, and 30.1 (ICDD No. 00-003-0227)) were clearer compared to those of the fresh catalyst, while the $NaWO_4$ peaks of the used catalyst were smaller relative to those of the fresh catalyst. The peaks of α-cristobalite and TiO_2, however, exhibited no substantial change. This might suggest that the crystallite size of α-tridymite could grow after many hours of testing. However, it has been reported that the change of α-cristobalite and α-tridymite does not substantially influence the activity of Na_2WO_4-MnO_x-containing catalysts for OCM reactions [32]. Thus, it is not only catalyst sintering that causes the gradual deactivation, but also the loss of Na_2WO_4.

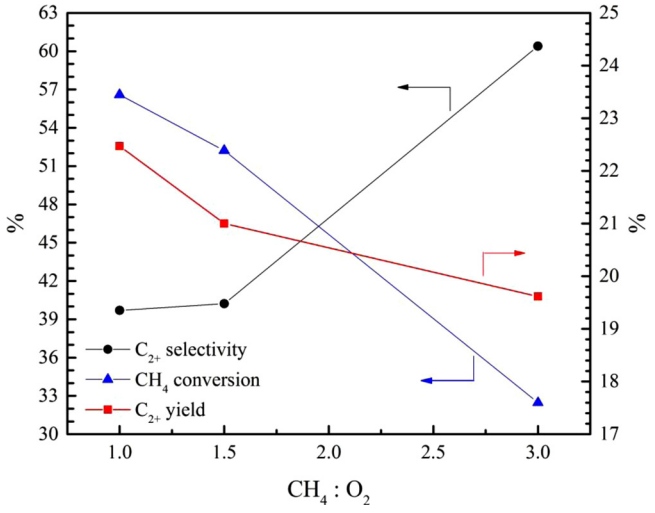

Fig. 10. Effect of varying CH_4:O_2 ratio of Na_2WO_4-Ti-Mn/SiO_2 catalyst. Reaction conditions: ($CH_4 + O_2$):N_2 ratio = 2:1, catalyst weight = 48 mg, total feed flow rate = 35 mL/min, reactor temperature = 700 °C.

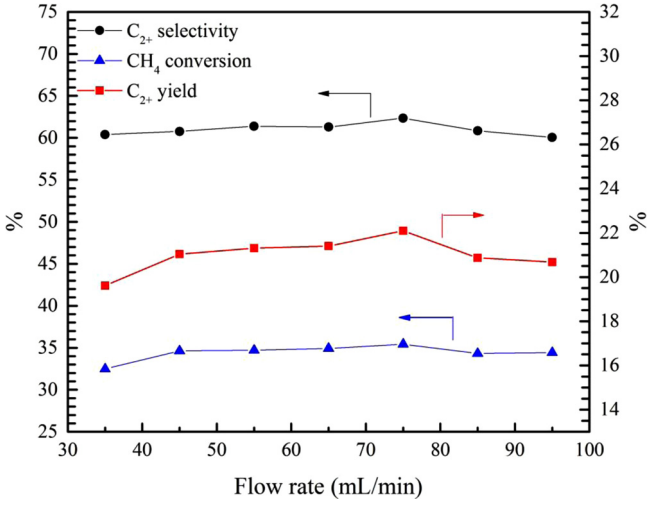

Fig. 11. Effect of varying total feed flow rate on catalytic performance of Na_2WO_4-Ti-Mn/SiO_2. Reaction conditions: CH_4:O_2:N_2 ratio = 3:1:2, catalyst weight = 48 mg, reactor temperature = 700 °C.

4. Conclusion

The purposes of this work were to study the effects of metal oxide additives on the performance of the TiO_2-Na_2WO_4/SiO_2 catalyst for the OCM reaction to value-added chemicals and to optimize the C_{2+} yield of the most promising catalyst. The plots between the CH_4 conversions and the binding energies of W $4f_{7/2}$ and Ti $2p_{3/2}$ of the prepared catalysts have revealed that the catalysts that exhibited lower binding energy values possessed high catalytic activity. This is because the bond strength between W or Ti with O becomes weaker, thereby promoting the OCM reaction. Moreover, the addition of Mn into the Na_2WO_4- Ti/SiO_2 catalyst was the most active catalyst. The crystalline phases of α-cristobalite, Na_2WO_4, and Mn_2O_3 were present in the most promising catalyst. In the attempts to optimize the C_{2+} yield by varying operating conditions, the maximum C_{2+} yield of the Na_2WO_4-Ti/SiO_2 catalyst added 0.5 wt% Mn was achieved at 22.09% with 62.3% C_{2+} selectivity and 35.43% CH_4 conversion. The optimal conditions were a reactor temperature of 700 °C, a CH_4:O_2:N_2 feeding gas ratio of 3:1:2, a total feed flow rate of 75 mL/min, and 48 mg of the catalyst. The stability of the catalyst was also investigated, concluding that the catalyst

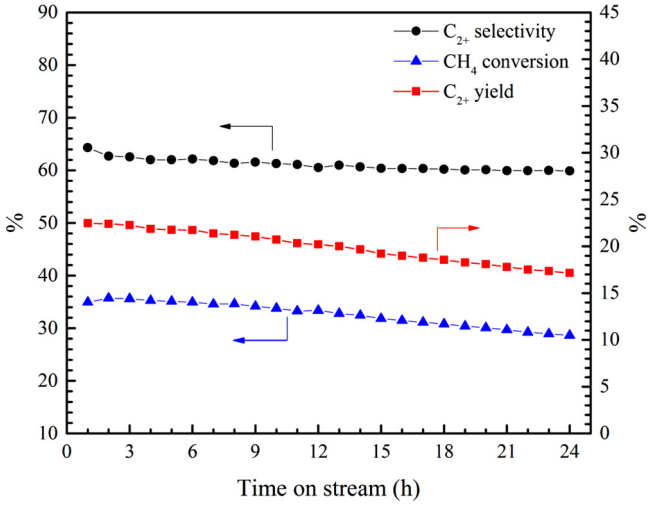

Fig. 12. Catalyst performance of Na_2WO_4-Ti-Mn/SiO_2 of OCM reaction as a function of time on stream over 24 h. Reaction conditions: CH_4:O_2:N_2 ratio = 3:1:2, catalyst weight = 48 mg, total feed flow rate = 75 mL/min, reactor temperature = 700 °C.

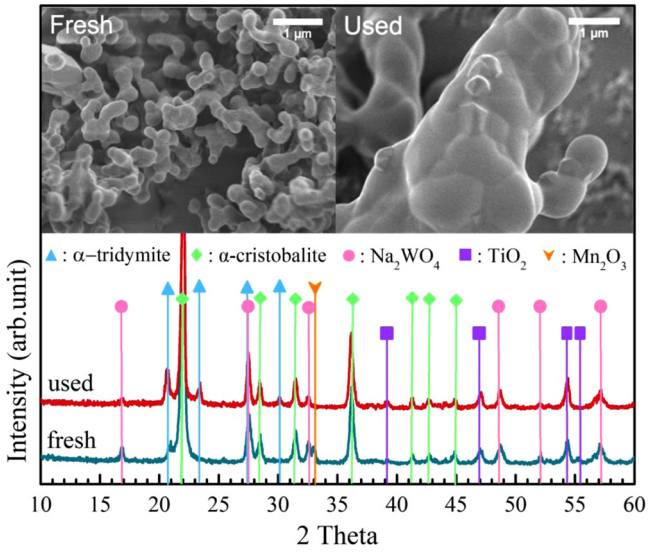

Fig. 13. SEM images (top) and XRD spectra (bottom) of fresh and used Na_2WO_2-Ti-Mn/SiO_2 catalyst.

gradually deactivated with time on stream because of catalyst sintering and the loss of Na_2WO_4 content. How to prevent catalyst deactivation and improve the C_{2+} selectivity of the Na_2WO_4-Ti-Mn/SiO_2 catalyst will be of great interest to further studies.

Acknowledgements

This work was financially supported by the Faculty of Engineering at Kasetsart University, Bangkok, Thailand; the Kasetsart University Research and Development Institute (KURDI); the Center of Excellence on Petrochemical and Materials Technology, the National Nanotechnology Center (NANOTEC), NSTDA, Ministry of Science and Technology, Thai- land, through its program of Research Network NANOTEC (RNN); the Thailand Research Fund and the Commission on Higher Education (grant #MRG6180232).

References

[1] C.D. Ruppel, J.D. Kessler, Rev. Geophys. 55 (2017) 126–168.

[2] G.J. Hutchings, M.S. Scurrell, J.R. Woodhouse, Chem. Soc. Rev. 18 (1989) 251–283.
[3] M.Y. Sinev, Z.T. Fattakhova, V.I. Lomonosov, Y.A. Gordienko, J. Nat. Gas Chem. 18 (2009) 273–287.
[4] M. Yildiz, Y. Aksu, U. Simon, T. Otremba, K. Kailasam, C. Göbel, F. Girgsdies, O. Görke, F. Rosowski, A. Thomas, R. Schomäcker, S. Arndt, Appl. Catal. A 525 (2016) 168–179.
[5] H.R. Godini, A. Gili, O. Görke, S. Arndt, U. Simon, A. Thomas, R. Schomäcker, G. Wozny, Catal. Today 236 (2014) 12–22.
[6] K. Khammona, S. Assabumrungrat, W. Wiyarath, J. Eng. Appl. Sci. 7 (2012) 447–455.
[7] S. Ji, T. Xiao, S. Li, L. Chou, B. Zhang, C. Xu, R. Hou, A.P.E. York, M.L.H. Green, J. Catal. 220 (2003) 47–56.
[8] J.Y. Lee, W. Jeon, J.W. Choi, Y.W. Suh, J.M. Ha, D.J. Suh, Y.K. Park, Fuel 106 (2013) 851–857.
[9] S.M.K. Shahri, A.N. Pour, J. Nat. Gas Chem. 19 (2010) 47–53.
[10] P. Wang, X. Zhang, G. Zhao, Y. Liu, Y. Lu, Chinese J. Catal. 39 (2018) 1395–1402.
[11] P. Wang, G. Zhao, Y. Liu, Y. Lu, Appl. Catal. A 544 (2017) 77–83.
[12] F. Papa, D. Gingasu, L. Patron, A. Miyazaki, I. Balint, Appl. Catal. A. 375 (2010) 172–178.
[13] V.H. Rane, S.T. Chaudhari, V.R. Choudhary, J. Nat. Gas Chem. 19 (2010) 25–30.
[14] N. Hiyoshi, T. Ikeda, Fuel Process. Technol. 133 (2015) 29–34.
[15] A. Seubsai, P. Tiencharoenwong, P. Kidamorn, C. Niamnuy, Eng. J. 23 (2019) 169–182.
[16] W. Kumsung, M. Chareonpanich, P. Kongkachuichay, S. Senkan, A. Seubsai, Catal. Commun. 110 (2018) 83–87.
[17] W.C. Liu, W.T. Ralston, G. Melaet, G.A. Somorjai, Appl. Catal. A 545 (2017) 17–23.
[18] S. Gu, H.S. Oh, J.W. Choi, D.J. Suh, J. Jae, J. Choi, J.M. Ha, Appl. Catal. A. 562 (2018) 114–119.
[19] T.W. Elkins, H.E. Hagelin-Weaver, Appl. Catal. A 497 (2015) 96–106.
[20] A. Malekzadeh, M. Abedini, A.A. Khodadadi, M. Amini, H.K. Mishra, A.K. Dalai, Catal. Lett. 84 (2002) 45–51.
[21] S.C. Oh, Y. Lei, H. Chen, D. Liu, Fuel 191 (2017) 472–485.
[22] V. Fleischer, R. Steuer, S. Parishan, R. Schomäcker, J. Catal. 341 (2016) 91–103.
[23] V. Fleischer, P. Littlewood, S. Parishan, R. Schomäcker, Chem. Eng. J. 306 (2016) 646–654.
[24] Y. Gambo, A.A. Jalil, S. Triwahyono, A.A. Abdulrasheed, J. Ind. Eng. Chem. 59 (2018) 218–229.
[25] A. Aseem, G.G. Jeba, M.T. Conato, J.D. Rimer, M.P. Harold, Chem. Eng. J. 331 (2018) 132–143.
[26] M. Ghiasi, A. Malekzadeh, S. Hoseini, Y. Mortazavi, A. Khodadadi, A. Talebizadeh, J. Nat, Gas Chem. 20 (2011) 428–434.
[27] C. Karakaya, H. Zhu, C. Loebick, J.G. Weissman, R.J. Kee, Catal. Today 312 (2018) 10–22.
[28] M. Taghizadeh, F. Raouf, Inorg. Nano-Met. Chem. 47 (2017) 1449–1456.
[29] Z. Gao, J. Zhang, R. Wang, J. Nat. Gas Chem. 17 (2008) 238–241.
[30] A. Galadima, O. Muraza, J. Ind. Eng. Chem. 37 (2016) 1–13.
[31] G. Pantaleo, V.L. Parola, F. Deganello, R.K. Singha, R. Bal, A.M. Venezia, Appl. Catal. B Environ. 189 (2016) 233–241.
[32] J. Wang, L. Chou, B. Zhang, H. Song, J. Zhao, J. Yang, S. Li, J. Mol. Catal. A Chem. 245 (2006) 272–277.